Lattice and central modes in the hyper-Raman spectra of the hydrogen-bonded ferroelectrics $PbHPO_4$ and $PbDPO_4$

S. Shin, Y. Tezuka, and M. Ishigame
Research Institute for Scientific Measurements, Tohoku University, 2-1-1 Katahira, Sendai, Miyagi 980, Japan

K. Deguchi and E. Nakamura
Department of Materials Science, Faculty of Science, Hiroshima University, Higashisenda-machi, Naka-ku, Hiroshima 730, Japan

(Received 1 September 1989; revised manuscript received 2 January 1990)

The hyper-Raman spectra of the hydrogen-bonded ferroelectrics $PbHPO_4$ (LHP) and $PbDPO_4$ are measured. The very weak intensity of the second-harmonic generation indicates that the space group of LHP in the paraelectric phase is centrosymmetric $P2/c$. The expected four $B_u(X,Y)$ lattice modes in the paraelectric phase are all observed by hyper-Raman scattering for both compounds, but they do not show the softening. Therefore, the softening mode that was observed in the ferroelectric phase is assigned to the A_g mode. On the other hand, the very strong relaxational central modes with B_u symmetry are found by hyper-Raman scattering for both compounds in the paraelectric phase. It is concluded that the phase transition in $PbHPO_4$ and $PbDPO_4$ is of the order-disorder type. The softening of the A_g lattice mode in the ferroelectric phase can be well elucidated by the coupling with the central mode for both compounds. The wave-vector dependence of the central mode shows that one-dimensional properties of $PbHPO_4$ are very weak.

I. INTRODUCTION

The hydrogen-bonded ferroelectrics $PbHPO_4$ (LHP) and its deuterated isomorph $PbDPO_4$ (DLHP) cause the ferroelectric phase transitions[1] around 310 and 452 K, respectively. This large isotope shift of phase-transition temperature (T_c) suggests that the proton dynamics plays an essential role in the phase-transition mechanism for LHP as well as for the other hydrogen-bonded ferroelectrics. Furthermore, the PO_4 ion group links one dimensionally by the hydrogen bonds along the c axis, as shown in Fig. 1, where the spontaneous polarization P_s is caused nearly along the direction of the hydrogen bond. Thus, it seems that LHP is one of the most suitable compounds to study the role of the proton dynamics on the isotope effect of T_c.

A lot of experiments have been performed in LHP, but many problems exist in the basic properties. The experimental results seem to be inconsistent with each other. First, the crystal structure in the high-temperature phase is not clear. Negran *et al.*[1] assumed that the space group is to be $P2/c$ (C_{2h}^4) in the paraelectric phase and Pc (C_2^2) in the ferroelectric phase. On the other hand, Nelmes *et al.*[2] reported that its crystal structure remains Pc above T_c, though their detailed studies for the crystal structure have not been reported. In fact, several experiments[2-5] suggested that it belongs to acentric Pc. However, the previous works of hyper-Raman scattering[6] and the second-harmonic-generation (SHG)[7] measurements show that the space group of LHP crystal belongs to centrosymmetric $P2/c$. Recently, Ermark *et al.*[8] reported that short-range ferroelectric order exists in the paraelectric phase due to the orientated defect in the crystal.

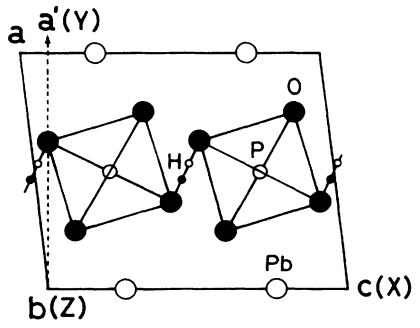

FIG. 1. Crystal structure of LHP projected onto the a-c plane. -●-○- denotes the hydrogen bond where a proton exists in either of the two sites.

Second, the type of soft mode related to the ferroelectric phase transition is not clear in LHP. The Raman spectra[2,4,9] show that the displacive-type softening mode exists clearly around 50–80 cm^{-1} in the ferroelectric phase of LHP [see Fig. 12(a)], though its softening is limited to about 50 cm^{-1} and the softening in DLHP (Refs. 3 and 4) is very little. This soft mode damps heavily with increasing temperature and disappears near T_c. The complex dielectric constant[10] in the gigahertz region also supported the same conclusion. In this sense, the phase transition of LHP is of a displacive type. However, Raman spectra[2-4] also show a relaxational mode as well as soft lattice mode. The recent complex dielectric measurements[11] of LHP and DLHP show the dielectric critical slowing down in the paraelectric phase. The hyper-Raman spectra[6] also show the relaxational-type central mode in the paraelectric phase. From the point of view

of the relaxational mode, LHP causes the order-disorder-type phase transition. As a result, two types of conflicting modes, that is, relaxational and soft lattice modes, coexist in LHP.

Third, there is no clear experimental evidence that LHP is a one-dimensional ferroelectric, though the hydrogen bond links one dimensionally in the crystal structure. Recent static dielectric measurements[11] show that the one-dimensional dielectric property is not found, though very slight deviation[12] from the Curie-Weiss law seems to exist.

In this study, we will examine the centrosymmetry of the crystal structures of LHP and DLHP by measuring the hyper-Raman spectra. We are also interested in the soft mode in the paraelectric phase by means of hyper-Raman scattering, because it has not been found in the paraelectric phase. If a softening lattice mode exists in the paraelectric phase, it is very interesting to know the relation between the softening lattice mode and the relaxational mode. Furthermore, it is more important to reveal the relation between the soft mode and the proton-tunneling mode. Because the symmetry of the ferroelectric soft mode related to the phase transition is $B_u(X,Y)$ in the paraelectric phase, this soft mode is active in hyper-Raman and inactive in Raman scattering. Thus, hyper-Raman scattering is the very suitable experimental technique for studying this mode. Next, one-dimensional dielectric properties will be examined by the wave-vector dependence of the central mode of LHP, which corresponds to the diffuse scattering measured by the neutron scattering around the Γ point, though it has not been performed so far. The wave-vector dependence of the central mode by means of the hyper-Raman scattering[13] has been successfully studied for the hydrogen-bonded ferroelectric CsH_2PO_4, because its one-dimensional property has been confirmed.

The unit cell of LHP is shown in Fig. 1. The factor-group analysis predicts $7A'(X,Y)+8A''(Z)$ optical lattice modes in the ferroelectric phase and $3A_g+4B_u(X,Y)+2A_u(Z)+6B_g$ modes in the paraelectric phase for LHP, as shown in Table I, if only the motions of Pb^{2+} and PO_4^{3-} are considered. On the other hand, proton modes are divided into $3B_u(X,Y)$ and $3A_u(Z)$ modes. The energy of the proton mode is generally higher than that of the lattice mode because of its light mass. However, the proton-tunneling mode becomes a soft mode and can exist in the low-frequency region of the lattice modes, when it couples with the lattice mode, as suggested in the phase-transition mechanism of KH_2PO_4 (KDP) by Kobayashi.[14] For LHP, the "ferroelectric soft mode" will be included in the $B_u(X,Y)$ modes for the paraelectric phase and in $A'(X,Y)$ modes for the ferroelectric phase, because the spontaneous polarization is caused in the a-c plain. Here, the "ferroelectric soft mode" means the softening lattice mode that causes the spontaneous polarization in the ferroelectric phase for the displacive-type phase transition and the polarization-fluctuation mode for the order-disorder-type phase transition. The Raman (A_g,B_g) and hyper-Raman (A_u,B_u) tensors in the paraelectric phase are given as follows:

$$A_g:\begin{bmatrix} a & d & 0 \\ d & b & 0 \\ 0 & 0 & c \end{bmatrix} \quad B_g:\begin{bmatrix} 0 & 0 & e \\ 0 & 0 & f \\ e & f & 0 \end{bmatrix} \quad B_u(X,Y):\begin{bmatrix} g & i & j & 0 & 0 & l \\ l & h & k & 0 & 0 & i \\ 0 & 0 & 0 & k & j & 0 \end{bmatrix} \quad A_u(Z):\begin{bmatrix} 0 & 0 & 0 & p & n & 0 \\ 0 & 0 & 0 & o & p & 0 \\ n & o & m & 0 & 0 & p \end{bmatrix}.$$

$A'(X,Y)$ and $A''(Z)$ modes in the ferroelectric phase are active in both Raman and hyper-Raman scattering;

$$A'(X,Y):\begin{bmatrix} a & d & 0 \\ d & b & 0 \\ 0 & 0 & c \end{bmatrix} \quad A''(Z):\begin{bmatrix} 0 & 0 & e \\ 0 & 0 & f \\ e & f & 0 \end{bmatrix} \quad A'(X,Y):\begin{bmatrix} g & i & j & 0 & 0 & l \\ l & h & k & 0 & 0 & i \\ 0 & 0 & 0 & k & j & 0 \end{bmatrix} \quad A''(Z):\begin{bmatrix} 0 & 0 & 0 & p & n & 0 \\ 0 & 0 & 0 & o & p & 0 \\ n & o & m & 0 & 0 & p \end{bmatrix}.$$

II. EXPERIMENT

Single crystals[11,12] of LHP and DLHP were grown at 40 °C by the gel method with tetramethoxysilane as the gel-forming agent. The deuteration rate of DLHP is estimated to be more than 96%. The optical quality of the crystals is very good, though they contain small inclusions in the center. Crystals were heated in air to 500 K for LHP and to 600 K for DLHP. There is no change in the optical quality of the LHP crystal. However, the DLHP crystal gradually becomes opaque at temperatures above 500 K for several hours. Though Lockwood *et al.*[2,3] reported the change in quality of LHP above 410 K, this change is not observed by us except for a very small anomaly at 410 K in the integrated intensity of the central modes and SHG (see $\log_{10}I_0$ around 410 K in Fig. 11). Ermark *et al.*[8] pointed out that the orientation of the defects exist in the crystal that was grown in the ferroelectric phase. However, the LHP crystals were grown in the paraelectric phase, so such defects do not seem to exist in this study.

Single crystals were cut into rectangular shapes of about $3\times6\times1$ mm^3 in LHP and $2\times3\times0.5$ mm^3 in DLHP. The direction of each face was parallel to each

TABLE I. Factor-group analysis of LHP.

$T<T_c$	$T>T_c$	Translational	Librational	H	Internal
$A'(X,Y)$	A_g	2	1		5
	$B_u(X,Y)$	2	2	3	4
$A''(Z)$	B_g	4	2		4
	$A_u(Z)$	1	1	3	5

crystallographic axis of c, a', and b, where a' is a pseudo-orthorhombic axis perpendicular to the b-c plane. All faces of these crystals were polished to give them optically flat surfaces. To define the polarization of hyper-Raman spectra, the orthogonal Cartesian-coordinate system X-Y-Z was used where X, Y, and Z axes were taken parallel to the crystal axes c, a', and b, respectively, as shown in the parentheses in Fig. 1.

An acoustic Q-switched neodymium-doped yttrium aluminum garnet (Nd-YAG) laser was used as a light source. The wavelength was 1.06 μm and the peak power of the pulse was about 20 kW at 1 kHz. The polarized laser beam with a single mode was focused into the sample by a lens of $f=100$ mm. A double-grating monochromator (Jasco, CT1000D) was used with a slit width of 100 μm that gave the resolution of about 1.2 cm^{-1}. As a detector, PIAS (photon-counting two-dimensional image acquisition system, Hamamatsu Photonics K.K.) was used. Since the intensity of the hyper-Raman-scattering light was very weak, a gated photon-counting system was also used to reduce the dark-count levels of the PIAS.

As a light source of the Raman scattering, SHG (532 nm) of the YAG laser was used. A $KTiOPO_4$ (KTP) crystal that was mounted on the kinematic bases was inserted into the optical pass of the YAG laser, in order to get the SHG exactly following the optical pass of the YAG laser. This light source[15] conveniently enabled us to use the same spectroscopic system that was used for the hyper-Raman measurement. A gated photon-counting system with a photomultiplier was used.

III. RESULTS AND DISCUSSION

A. Lattice modes

Figure 2 shows the Raman spectra of LHP that are measured at 296 K in the ferroelectric phase and at 315 and 363 K in the paraelectric phase. Two prominent A_g bands are seen around 100 and 172 cm^{-1}. These Raman spectra are consistent with the results of Lockwood *et al.*[2] It should be noted that the last A_g band is not found, though the three A_g bands are anticipated by the factor-group analysis. The several small structures found in the spectra are the leaked modes that have different symmetries. The structures marked by the asterisk belong to the B_g modes and the structure marked by the vertical line is the B_u mode, as discussed later. At the lower teperature, a prominent structure is found at around 77 cm^{-1} in the Raman spectra[2] [see Fig. 12(a)]. This structure has the characteristic temperature dependence that its frequency becomes softened and its width becomes wide toward T_c.

On the other hand, the $B_u(X,Y)$ lattice modes are measured at 315 K for the three scattering configurations $Y(XX,X)Z$, $Z(YY,Y)X$, and $Y(ZZ,X+Y)Z$ by hyper-Raman scattering, as shown in Fig. 3, where the first two letters in the parentheses denote polarizations of the two incident photons and the third is the polarization of the scattered photon. The abscissa is the frequency shift from $2\omega_0$, where ω_0 is the frequency of the incident laser beam. As shown in $Y(XX,X)Z$ configuration in Fig. 3, the four lattice modes are clearly seen at 114, 142, 161, and 207 cm^{-1}. In the case of the $Z(YY,Y)X$ configuration, the structure at 114 cm^{-1} is shifted to that at 106 cm^{-1}. A very weak and broad structure is seen around 250 cm^{-1}. Since the structures at 161 and 207 cm^{-1} are not found in the $Z(YY,Y)X$ configuration, they have the polarization parallel to the $c(X)$ axis and the structures at 114 and 142 cm^{-1} have the polarization parallel to the $a'(Y)$ axis. These four $B_u(X,Y)$ lattice modes in the hyper-Raman spectra partly correspond to the lattice modes assigned by the infrared[16] and Raman[2] measurements in the ferroelectric phase, as shown in Table II. However, the soft lattice mode around 77 cm^{-1} that is assigned to the $B_u(X,Y)$ mode by the Raman[2] and infrared[16] measurements cannot be found in hyper-

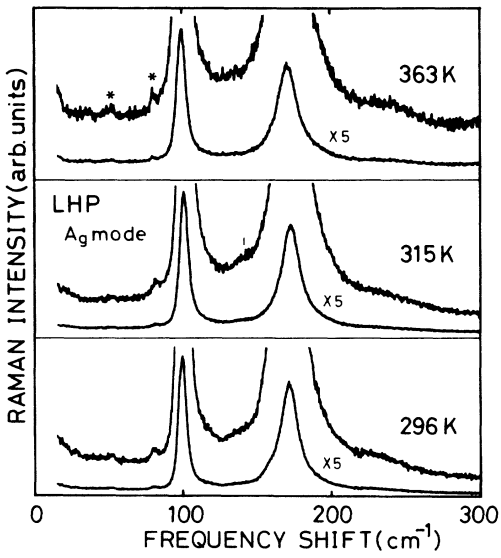

FIG. 2. Temperature dependence of the A_g lattice modes measured by Raman scattering in the $Y(XX)Z$ configuration. Structures marked by an asterisk are the leaked B_g modes. The structure marked by the tic mark is the $B_u(X,Y)$ mode.

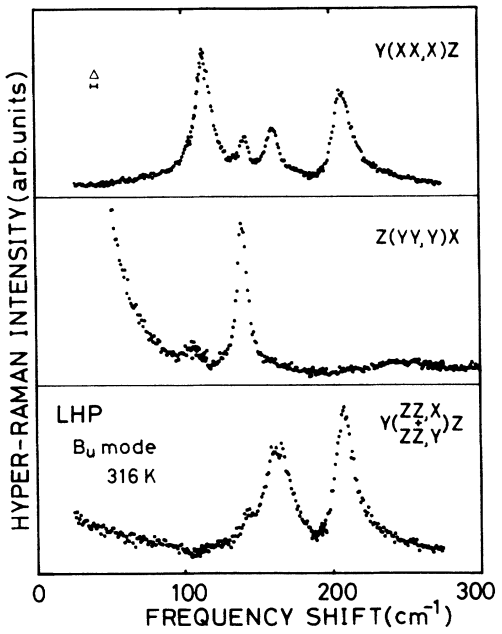

FIG. 3. The hyper-Raman spectra measured in three different $B_u(X,Y)$ configurations at 316 K.

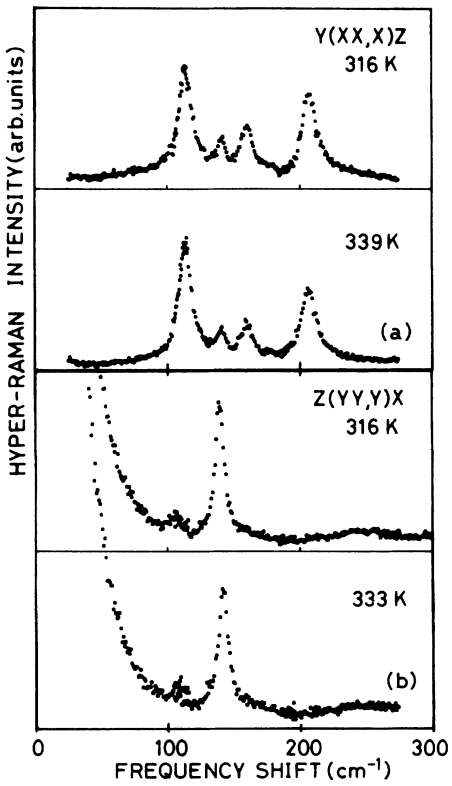

FIG. 4. Temperature dependence of the $B_u(X,Y)$ lattice modes of LHP measured in the $Y(XX,X)Z$ and $Z(YY,Y)X$ configurations.

Raman spectra at all.

Figure 4 shows the temperature dependence of the $B_u(X,Y)$ lattice modes. Since the prominent frequency shift cannot be found, the softening lattice mode does not exist in the paralelectric phase, in contrast to the Raman spectra[2] in the ferroelectric phase. The extremely broad band at 244 cm^{-1} becomes a little stronger at the high temperature, so that this mode will be the higher harmonics. This structure becomes much stronger in the hyper-Raman spectrum of DLHP at 490 K.

Figure 5 shows the $B_u(X,Y)$ lattice modes of DLHP in the paraelectric phase measured at 490 K by hyper-Raman scattering. The lattice modes are seen at 114, 138, 157, and 203 cm^{-1}, which have a lower frequency by about 4 cm^{-1} than those of LHP. Thus, these four $B_u(X,Y)$ modes are not proton-tunneling modes, since the prominent isotope shift does not exist.

The four $B_u(X,Y)$ lattice modes that are anticipated by the factor-group analysis are entirely found in the hyper-Raman spectra. Furthermore, these modes are not ferroelectric soft modes. If the 77-cm^{-1} soft mode belongs to the B_u mode, this mode should be found in the hyper-Raman spectra. However, this mode cannot be observed by hyper-Raman scattering. Therefore, it is concluded that the symmetry of this soft mode in the Raman spectra is not $B_u(X,Y)$ and should be assigned to the A_g mode. The structures at 100 and 172 cm^{-1} have always been assigned to the A_g modes in the Raman and infrared measurements. However, the last A_g mode has

TABLE II. The assignments of the $4B_u(X,Y)$ and $3A_g$ lattice modes of LHP by means of hyper-Raman scattering at 316 K in the $Y(XX,X)Z$ configuration, Raman measurements (Ref. 2) at 315 and 10 K in the $Y(XX)Z$ configuration, and infrared measurements (Ref. 16) at 4 K. No structure can be found in the energy regions labeled by an asterisk, though a structure has been found by other measurements.

Hyper-Raman 316 K	Raman 315 K	$>T_c>$	Raman (Ref. 2) 10 K		Infrared (Ref. 16) 4 k	
*	*		77 (B_u)		79 [$B_u(c)$]	
	100 (A_g)			102 (A_g)		100 (A_g)
114 [$B_u(a)$]			122 (B_u)		112 [$B_u(a)$]	
142 [$B_u(a)$]			147 (?)		148 [$B_u(a)$]	
	*			165 (A_g)		*
161 [$B_u(c)$]			171 (B_u)		168 [$B_u(c)$]	
	172 (A_g)			178 (A_g)		187 (A_g)
207 [$B_u(c)$]			229 (B_u)			229 (A_g)

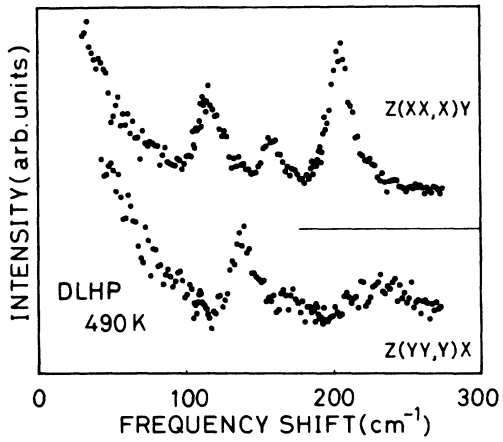

FIG. 5. The $B_u(X,Y)$ lattice modes of DLHP measured by hyper-Raman scattering at 490 K in the $Z(XX,X)Y$ and $Z(YY,Y)X$ configurations.

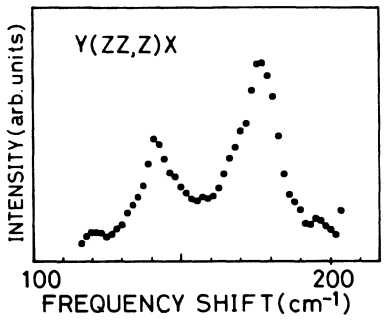

FIG. 6. The $A_u(Z)$ lattice modes measured by hyper-Raman scattering at 316 K.

not been definitely found in the paraelectric phase by Raman scattering. From the measurement of the Raman scattering[2] at 10 K, the very weak structure at 164.6 cm^{-1} has been assigned to the last A_g mode. However, this structure can be seen only in the $Y(XX)Z$ configuration and cannot be seen in the infrared measurement,[16] so that this structure may be associated with impurities or may be a combination band as is often seen weakly in the polarized Raman spectrum. Though the structure at 229 cm^{-1} has been assigned to the last A_g mode by means of infrared measurement,[16] this mode has been assigned to the $B_u(X,Y)$ mode by Raman and hyper-Raman measurements. Therefore, if the 77-cm^{-1} structure belongs to the A_g mode, the assignments of the other structures by means of all three measurements become consistent with each other.

The infrared[16] and Raman[2] measurements show that the direction of polarization by this softening lattice mode is along the c axis in the ferroelectric phase rather than the a' axis. On the contrary, the direction of spontaneous polarization is almost along the a' axis. This fact suggests that this softening mode is not directly related to the ferroelectric phase transition.

In the Raman spectra shown in Fig. 2, a $B_u(X,Y)$ mode is slightly seen around 140 cm^{-1} even in the paraelectric phase. This fact has been already suggested by Lockwood *et al.*[2] From this fact, they concluded that the crystal structure does not change through the phase transition. However, the SHG measurements[6,7] (see also Sec. III B) clearly show that the crystal structure in the paraelectric phase has centrosymmetry, while that in the ferroelectric phase does not have centrosymmetry. From the point of view of the order-disorder phase transition, the structure belonging to the ordered phase is often seen even in the disordered phase, because the disordered "microdomains" that do not have a real inversion center appear momentarily in the paraelectric phase. These "microdomains" appear according to the ferroelectric correlation length that is decided by the statistical mechanics. For example, it is well known that the infrared active modes appear in the paraelectric Raman spectra[17] of $NaNO_2$, whose phase transition is of the order-disorder type. In the case of internal modes, the forbidden-infrared-active modes have been observed in the Raman spectra very often.[18]

The two $A_u(Z)$ modes of LHP are seen at 141 and 177 cm^{-1} for $Y(ZZ,Z)X$ configuration, as shown in Fig. 6. These structures are consistent with the results of the infrared-absorption measurements.[16]

B. Central modes

Figure 7 shows the hyper-Raman spectra of LHP in the energy region of the SHG and the central mode. The SHG scattering that has the same linewidth as the resolution cannot be seen near T_c and is weakly seen at high temperatures far above T_c. It is clear that the crystal

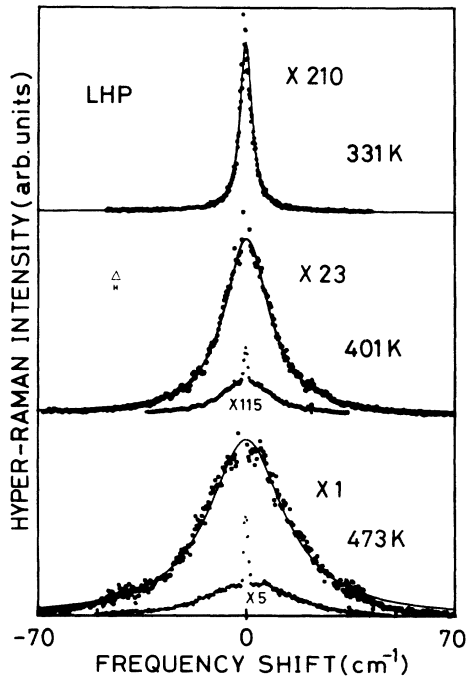

FIG. 7. The transverse central mode observed by hyper-Raman scattering of LHP in the $Z(YY,Y)X$ configuration.

structure of LHP has centrosymmetry. That is, the space group of LHP is $P2/c$ in the paraelectric phase. Since the SHG intensity of LHP is as weak as that of the "perfect" ionic crystals in the hyper-Raman spectra,[19] the optical quality of LHP is found to be very good. The weak SHG may be caused by the defects that cannot be removed in the crystal.

The central modes of LHP are very strong compared with the lattice modes. It is found that the peak intensity of the central mode drastically increases and its half-width becomes narrow as the temperature decreases toward $T_c = 310$ K.

The central modes of DLHP are also shown in Fig. 8. The linewidth is much narrower than that of LHP. The SHG intensity of DLHP is also very weak.

The central mode does not become an underdamped phonon even at very high temperatures far above T_c. Each central mode is well fitted by a Lorentzian, as shown by the solid line in Figs. 7 and 8. Therefore, the central mode can be represented by the relaxational mode whose line shape is given by

$$I(\omega) \sim \frac{kT}{\hbar}\chi(0)\frac{\tau}{1+(\omega\tau)^2} . \quad (1)$$

Here, τ is the relaxation time. In the previous hyper-Raman study,[6] the line-shape analysis of $I(\omega)\omega^2$ has shown that the central mode of LHP is the relaxational mode (see Fig. 4 in Ref. 6). In this study, the line-shape analyses are performed in LHP and DLHP at very high temperatures, leading to confirm again that the central mode is the relaxational mode (the figures are not shown).

In the paraelectric phase of LHP, the soft lattice mode does not exist and the very strong relaxational mode does exist. Therefore, it is concluded that the phase transition in LHP and DLHP is of the order-disorder type.

Since each central mode is well fitted by a single Lorentzian, the distribution of the relaxation time is very narrow. This result is consistent with that of the dielectric measurement.[11]

The small solid circles in Fig. 9 are the inverse relaxation times, τ^{-1} that are obtained by the half-width of the Lorentzian fitted to the central modes of LHP. It is found that the temperature dependence of τ^{-1} is in proportion to the temperature as $\tau = \tau_0 T_c/(T-T_c)$, where $\tau_0 = 1.6\times10^{-13}$ sec and $T_c = 310$ K, as shown by the solid line of Fig. 9. Therefore, the temperature dependence of τ^{-1} of LHP follows the Curie-Weiss law. Thus, the one-dimensional dielectric properties seem to be weak in LHP, if any, because the deviation from the Curie-Weiss law cannot be observed. The estimated τ_0 are very similar to those obtained by infrared[20] and dielectric[11] measurements, as seen in Table III.

The open circles in Fig. 9 also show the relaxation time of DLHP. The solid line is $\tau = \tau_0 T_c/(T-T_c)$, where $\tau_0 = 4.5\times10^{-13}$ sec, and $T_c = 457$ K. The DLHP crystal becomes opaque at high temperatures. Therefore, the relaxation times may deviate from the Curie-Weiss law at high temperatures. In the case of $\chi(0)$, which will be discussed later (see T/I_0 in Fig. 11), the measuring time is short, so that the crystal quality may not be changed and $\chi(0)$ of DLHP well follows the Curie-Weiss law in contrast to τ.

In the ferroelectric phase, relaxational central modes become Raman active. In fact, relaxational central modes are observed in the Raman spectra.[2,3] The τ_0 that is evaluated from these Raman spectra[4] for LHP and DLHP in the temperature region around T_c is consistent

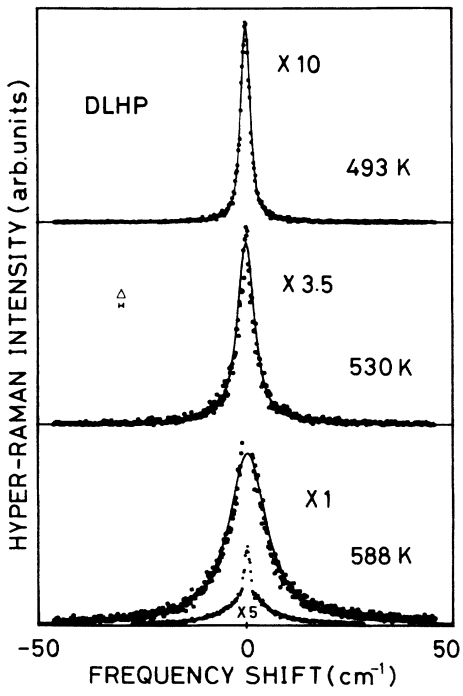

FIG. 8. The transverse central mode observed by hyper-Raman scattering of DLHP in the $Z(YY,Y)X$ configuration.

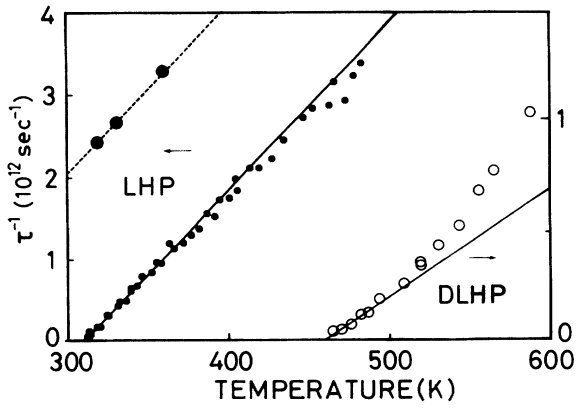

FIG. 9. Relaxation times of LHP for the transverse central mode (small solid circles) and the longitudinal-mixed central mode (large solid circles) measured by hyper-Raman scattering. The solid line is $\tau = 1.6\times10^{-13}\ T_c/(T-T_c)$ sec, where T_c is 310 K. The dashed line is $\tau = 1.6\times10^{-13}\ T_c/(T-T_c+LT_c/2)$ sec, where the depolarization field LT_c is 220 K. Open circles are the relaxation times of DLHP for the transverse central mode. The solid line is $\tau = 4.5\times10^{-13}\ T_c/(T-T_c)$ sec, where T_c is 457 K.

TABLE III. The relaxation times of an isolated dipole, τ_0 (10^{-13} sec), in LHP and DLHP.

		Infrared (Ref. 20)	Dielectric (Ref. 11)	Hyper-Raman
LHP	$T<T_c$	0.42		
	$T>T_c$	1.7	1.9	1.6
DLHP	$T<T_c$			
	$T>T_c$		2.5	4.5

with the τ_0 that is obtained by the other experimental methods as shown in Table III. However, it is curious that the relaxational modes in the Raman spectra[2-4] do not obey the Curie-Weiss law.

As shown in Fig. 3, the very strong central mode centered at 0 cm^{-1} is clearly observed in the $Z(YY,Y)X$ configuration. However, in the case of the $Y(ZZ,X+ZZ,Y)Z$ configuration, the central mode is very broad and weak. On the other hand, in the $Y(XX,X)Z$ configuration, the central mode cannot be found. That is, the central mode has the very strong configuration dependence. Since the direction of spontaneous polarization is nearly along the $a'(Y)$ axis,[21] the central mode is strong in the $Z(YY,Y)X$ configuration, where Y polarization is caused, while the central mode is absent in the $Y(XX,X)Z$ configuration, where X polarization is caused.

Because the central mode is the polarization-fluctuation mode, both transverse and longitudinal modes exist in the central mode. Figure 10 shows the central modes in the $Y(ZZ,Y)Z$ configuration. This spectrum is the longitudinal-mixed central mode, while Figs. 7 and 8 show the transverse central mode. The half-width of the longitudinal-mixed central mode is much broader than that of the transverse one and its intensity is much weaker. The large solid circles in Fig. 9 represent the temperature dependence of τ^{-1} for the longitudinal-mixed central mode, which also follows the Curie-Weiss law, $\tau^{-1}=C/(T-T_c')$. The parameter C is the same value as that in the case of the transverse configuration. However, T_c' is 200 K, which is very different from $T_c=310$ K.

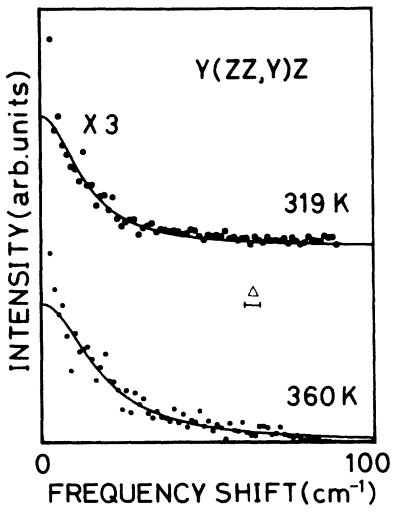

FIG. 10. The longitudinal-mixed central mode observed by hyper-Raman scattering of LHP in the $Y(ZZ,Y)Z$ configuration.

It is known that the central mode has a wave-vector dependence due to the depolarization field, when it is caused by the polarization fluctuation. In this case, $\chi(0,q)$ is written as follows:[22]

$$\chi(0,q)\sim\frac{1}{T-T_c+LT_c(q_z/q)^2}\ . \tag{2}$$

It is known that $\chi(0,q)$ is proportional to $\tau(q)$. Thus, the depolarization field LT_c of LHP is obtained to be 220 K (dashed line in Fig. 9). For KDP, which is a three-dimensional ferroelectric, LT_c was evaluated to be 60–90 K.[22,23] On the other hand, LT_c of CsH_2PO_4 (CDP), which is one-dimensional ferroelectric, is evaluated to be 1555 K.[13] In the case of the one-dimensional ferroelectrics, LT_c is large, becuase the anisotropy due to the one-dimensional correlation length enlarges the LT_c value. Thus, since LT_c is not so large in LHP, it is found that the one-dimensional correlation length in LHP is small.

However, there is a problem with determining the origin of the polarization fluctuation. The structure analyses by means of x ray and neutron scattering are not sufficient for LHP. Therefore, we tentatively assume the distorted PO_4 ions, each of which has a permanent dipole moment for the origin of the polarization fluctuation. This mechanism has been supposed for the KDP (Ref. 24) and CDP (Ref. 25).

The temperature dependences of the total intensity I_0 of the central mode and SHG are measured with the spectral resolution of 100 cm^{-1}, as shown in the lower parts of Fig. 11 for LHP and DLHP. Most of the intensity above T_c results from the central mode because the intensity of SHG is weak as shown in Figs. 7 and 8. However, most of the intensity below T_c is due to SHG, because SHG is allowed in the ferroelectric phase. It is known that I_0/T for the central mode is in proportion to the susceptibility $\chi(0)$. One can see that the $\chi(0)$ follows the Curie-Weiss law $\chi^{-1}(0)\sim T-T_c$ above T_c for LHP and DLHP rather than the quasi-one-dimensional static susceptibility,[26-29] as shown in the upper part of Fig. 11.

On the other hand, one can find that I_0 is proportional to T_c-T in $T<T_c$, as shown in Fig. 11. It is empirically known[30] that the intensity of SHG is proportional to the spontaneous polarization P_s. Therefore, it is concluded

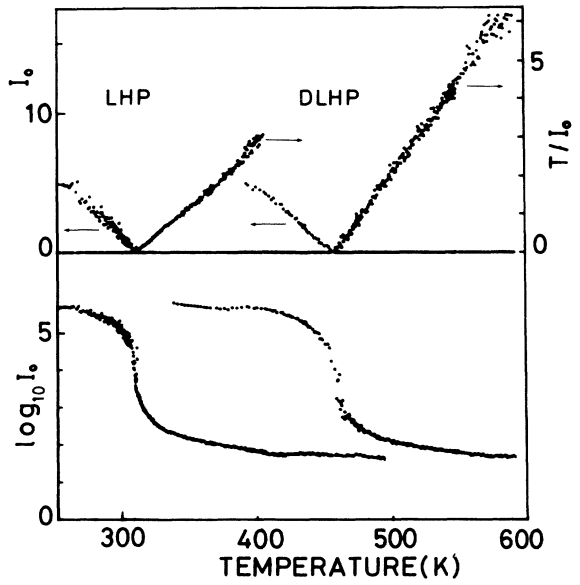

FIG. 11. Temperature dependence of the total intensity I_0 of the SHG and the central mode for LHP and DLHP. I_0 below T_c corresponds to the spontaneous polarization P_s. T/I_0 above T_c corresponds to the inverse susceptibility $\chi^{-1}(0)$.

that $P_s \sim T_c - T$ below T_c in LHP and DLHP. Of course, when the temperature is far below T_c, the intensity of SHG is varied with temepratures mainly according to the phase-matching relation because the refractive index has a temperature dependence. Smuty and Fousek[31] have measured P_s, whose temperature dependence is consistent with our hyper-Raman results. The I_0 and T/I_0 become zero from below and above T_c, respectively, and are smoothly connected to each other at T_c, as seen in Fig. 11. This fact suggests that the phase transition of LHP and DLHP is of second order.

C. Coupling between the lattice and the central modes

Generally, the lattice mode that has the lowest vibrational energy can be coupled more or less with the central mode, when both modes belong to the same symmetry. For CDP, this type of coupling has been studied in detail by means of hyper-Raman scattering.[13] As for the $Z(YY,Y)X$ configuration of LHP, the lattice mode at 106 cm^{-1} is shifted to the lower energy than those of the other configurations by about 10 cm^{-1}. Because the central mode is extremely strong in this configuration, the softening of the lattice mode is caused due to the coupling with the central mode. However, the temperature dependence of this softening is not so large, as shown in Fig. 4(b). This fact shows that this coupling is not directly related with the phase transition.

In the case of the ferroelectric phase of LHP, the central mode becomes Raman-active. In fact, the central mode is found in Raman scattering,[2] though its intensity is not so strong as in the hyper-Raman scattering. Therefore, the $A'(X,Y)$ lattice mode, which is the A_g mode in the paraelectric phase, can be coupled with the central mode in the ferroelectric phase. The lattice mode around 77 cm^{-1} may be strongly coupled with the central mode, because this mode has the lowest energy among all the $A'(X,Y)$ lattice modes. As the microscopic coupling mechanism is not known, we use the simplest coupling form, as follows:

$$\chi(\omega,T)^{-1}=\omega_0^2-\omega^2-i\omega\gamma-\frac{\delta^2(T)}{1-i\omega\tau(T)}\ , \tag{3}$$

where δ is a coupling constant and taken as

$$\delta^2(T)=\begin{cases}220\,000/(T_c-T), & T<T_c-45\ \text{K}\\ \text{const}, & T>T_c-45\ \text{K}\end{cases}$$

$$\omega_0=84\ cm^{-1}\ ,$$

$$\tau(T)=2.5\times10^{-12}/(T_c-T)\ \text{sec}\ ,$$

$$\gamma=0\ .$$

Figure 12(b) is the example of the calculated results and Fig. 12(a) shows the Raman spectra measured by Lockwood *et al.*[2] As shown in Fig. 12, the softening and the broadening of the phonon are well elucidated by the coupling. Therefore, it is concluded that the anomalous temperature dependence of this mode is caused by the coupling with the central mode.

Figure 13 shows the Raman spectra[3] of DLHP and

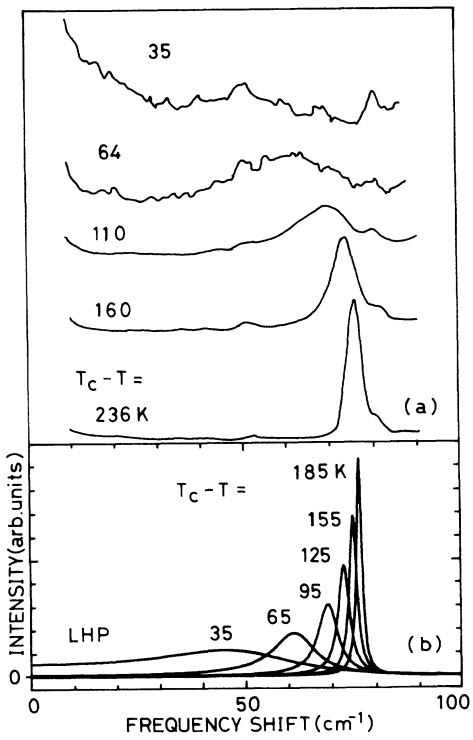

FIG. 12. (a) The softening mode of LHP in the ferroelectric phase that was measured by the Raman scattering in the $Y(XX+XY)Z$ configuration (Ref. 2). (b) The example of the calculation of the A_g lattice mode that is softened by the coupling with the central mode.

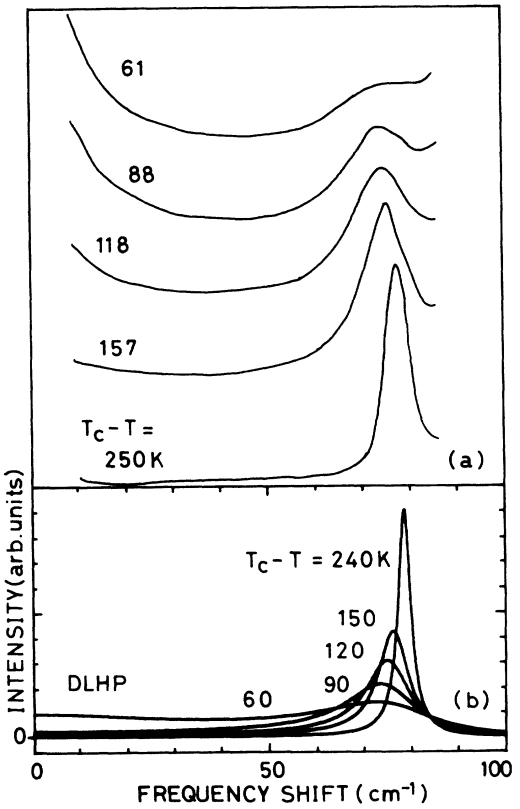

FIG. 13. (a) The softening mode of DLHP in the ferroelectric phase that was measured by the Raman scattering in the $Y(XX)Z$ configuration (Ref. 3). (b) The example of the calculation of the A_g lattice mode that is softened by the coupling with the central mode.

their calculated results. The used parameters are the same as those of LHP except $\tau(T)=1.0\times10^{-11}/(T_c-T)$ sec, which is longer than that of LHP. This fact shows that the coupling mechanism of LHP and DLHP is the same. Because the central mode of DLHP is narrow, the softening of the lattice mode is not so large.

In the ferroelectric phase, $\tau(T)$ of LHP has been also obtained by the Brillouin[32] and infrared[20] measurements to be $9.33\times10^{-11}/(T_c-T)$ sec and $1.3\times10^{-11}/(T_c-T)$ sec, respectively. However, the evaluated values are different from each other. Since longitudinal-mixed relaxation modes are measured by the Raman-scattering configuration,[2] $\tau(T)$ is shorter than that of the transverse relaxation time, which is measured by infrared measurements.

The physical origin of the temperature dependence of the coupling constant $\delta(T)$ cannot be understood. However, it is clear that this lattice mode takes part in the phase transition anyway. We think that this softening lattice mode may be the librational mode, because the librational motion between the PO_4 ions is more easily coupled with the central mode that is caused by the fluctuation of the distorted PO_4 ion, rather than the translational mode.

However, there is a serious problem. That is, this A_g mode is missing in the paraelectric phase in all Raman-scattering configurations,[2] though this band is clearly seen in the ferroelectric phase. The detailed mechanism has not been understood yet. However, since the polarization fluctuation is very fast in this material, the relaxation time of the distortion of PO_4 ions is expected to be fast. Therefore, the lifetime of the librational motion of PO_4 ions may be too short to make a phonon frequency. The existence of such a "missing" mode in the paraelectric phase has been already known in KDP. In KDP, the A_1 librational mode that is coupled with the relaxational central mode is found in the ferroelectric phase by Raman measurements.[33] However, in the case of the paraelectric phase, this mode cannot be found in the A_1 configuration.[34] It is surprising that this A_1 librational mode appears with strong intensity in the $B_2(Z)$ configuration, if the Tominaga's assignment[24,35] is true. Moreover, in the case of the hyper-Raman measurements of KDP,[15] this A_1 librational mode has not been found in any configuration. In contrast to KDP, the "missing" mode in the paraelectric phase of LHP could not be found in any configuration and any light-scattering method.

It is well known that hydrogen-bonded ferroelectrics have prominent isotope effect on T_c. However, the phase-transition mechanism has not been settled irrespective of a lot of theoretical and experimental efforts.[36,37] An important problem is determining how much the proton tunneling plays a role in the phase-transition mechanism. However, since the proton-tunneling mode has not been experimentally found, the dynamics of the proton have not been able to be understood. The phase transition of LHP is found to be caused by the polarization fluctuation of distorted PO_4 ions, so that the proton dynamics must be coupled with this polarization fluctuation, if the proton participates in the phase-transition mechanism. Such a mechanism was proposed for CDP (Ref. 38) and successfully elucidated the isotope effect on T_c. We think that the librational mode is closely coupled with the protonic motion, namely tunneling or hopping to the other site in the double well of the hydrogen bond, because the librational motion varies the O—H · · · O distance. The shortening of the O—H · · · O distance may bring about the proton tunneling. In the phase-transition mechanism of LHP, the coupling among the proton dynamics between PO_4 ions, librational motion of PO_4 ions, and the polarization fluctuations due to the distorted PO_4 ions may be important.

IV. CONCLUSION

Irrespective of the prominent isotope effect on T_c, the proton-tunneling mode cannot be found in LHP and DLHP. It is concluded that LHP and DLHP cause the typical order-disorder phase transition, because hyper-Raman spectra show the very strong-relaxational-type central modes and any softening lattice mode cannot be found in the paraelectric phase. The temperature dependence of the central mode follows the Curie-Weiss law well. The wave-vector dependence of the central mode

suggests that LHP is rather a three-dimensional ferroelectric, irrespective of the one-dimensional network of the hydrogen bonds and PO_4 ions.

It is found that the softening lattice mode that was observed in the ferroelectric phase by Raman scattering belongs to the A_g mode. The softening of the lattice mode in the ferroelectric phase can be well elucidated for both LHP and DLHP by the calculation of the coupling with the central mode. The softening of the lattice mode in DLHP is little because of the narrow width of the central mode. However, in the paraelectric phase, this mode is missing in both Raman and hyper-Raman spectra. The similarity between this A_g lattice mode of LHP and the A_1 librational mode of KDP is suggested because they are missing in the paraelectric phase and become softened due to the coupling with the relaxational central modes in the ferroelectric phase.

Since the SHG intensity is very weak, it is clear that the space group of LHP and DLHP in the paraelectric phase is centrosymmetric $P2/c$.

[1]T. J. Negran, A. M. Glass, C. S. Brickenkamp, R. D. Rosenstein, R. K. Osterheld, and R. Susott, Ferroelectrics **6**, 179 (1974).

[2]D. J. Lockwood, N. Ohno, R. J. Nelmes, and H. Arend, J. Phys. C **18**, L559 (1985); N. Ohno and D. J. Lockwood, J. Chem. Phys. **83**, 4374 (1985); D. J. Lockwood, N. Ohno, and M. H. Kuok, J. Phys. C **20**, 3751 (1987).

[3]D. J. Lockwood, N. Ohno, M. H. Kuok, and H. Arend, J. Phys. C **19**, L233 (1986); N. Ohno, D. J. Lockwood, and M. H. Kuok, J. Chem. Phys. **84**, 6599 (1986); N. Ohno, D. J. Lockwood, and M. H. Kuok, J. Phys. C **20**, 1599 (1987).

[4]N. Ohno and D. J. Lockwood, Ferroelectrics **72**, 1 (1987); N. Ohno and D. J. Lockwood, Ferroelectrics **94**, 361 (1989).

[5]A. Keens and H. Happ, J. Phys. C **21**, 1661 (1988).

[6]S. Shin, M. Ishigame, K. Deguchi, and E. Nakamura, Solid State Commun. **65**, 749 (1988).

[7]M. Zgonik, M. Copic, and H. Arend, J. Phys. C **20**, L565 (1987).

[8]F. Ermark, B. Topic, U. Haeberlen, and R. Blinc, J. Phys. Condens. Matter **1**, 5489 (1989).

[9]B. B. Lavrencic and J. Petzelt, J. Chem. Phys. **67**, 3890 (1977).

[10]H. Happ, D. Langhardt, and G. Voss, J. Phys. C **19**, 2575 (1986).

[11]K. Deguchi and E. Nakamura, J. Phys. Soc. Jpn. **57**, 413 (1988).

[12]N. Nakatani, J. Phys. Soc. Jpn. **56**, 2542 (1987).

[13]S. Shin and M. Ishigame, Phys. Rev. B **37**, 2718 (1987).

[14]K. K. Kobayashi, J. Phys. Soc. Jpn. **24**, 497 (1968).

[15]S. Shin, A. Sugawara, Y. Tezuka, and M. Ishigame, Solid State Commun. **71**, 685 (1989).

[16]E. J. Kock and H. Happ, Phys. Status Solidi B **97**, 239 (1980).

[17]C. M. Hartwig, E. Wiener-Avnear, and S. P. S. Porto, Phys. Rev. B **5**, 79 (1972); F. Brehat and B. Wyncke, J. Phys. C **18**, 1705 (1985); A. D. Prasad-Rao and S. P. S. Porto, in *Light Scattering in Solids,* edited by M. Balkanski, R. C. C. Leite, and S. P. S. Porto (Flammarion, Paris, 1976), p. 877.

[18]Y. Tominaga, H. Urabe, and M. Tokunaga, Solid State Commun. **48**, 265 (1983); B. Marchon and A. Novak, J. Chem. Phys. **78**, 2105 (1983); M. Aoki, M. Kasahara, and I. Tatsuzaki, J. Raman Spectrosc. **15**, 97 (1984).

[19]H. Vogt and H. Presting, Phys. Rev. B **31**, 6731 (1985); H. Vogt and G. Neumann, Phys. Status Solidi B **92**, 57 (1979); S. Shin and M. Ishigame, Phys. Rev. B **34**, 8875 (1986).

[20]J. Kroupa, J. Pezelt, G. V. Kozlov and A. A. Volkov, Ferroelectrics **21**, 387 (1978).

[21]N. Nakatani, Jpn. J. Appl. Phys. **24**, Suppl. 24-2, 948 (1985).

[22]M. Tokunaga, J. Phys. Soc. Jpn. **50**, 3009 (1981).

[23]M. Sawafuji, M. Tokunaga, and I. Tastuzaki, J. Phys. Soc. Jpn. **47**, 1860 (1979); **47**, 1870 (1979).

[24]For examples, M. Tokunaga and I. Tatsuzaki, Phase Transitions **4**, 97 (1984); M. Tokunaga and T. Matsubara, Ferroelectrics **72**, 175 (1987), and references therein.

[25]See references in Ref. 38.

[26]S. Shin, A. Ishida, T. Yamakami, T. Fujimura, and M. Ishigame, Phys. Rev. B **35**, 4455 (1987).

[27]K. Deguchi, E. Okaue, and E. Nakamura, J. Phys. Soc. Jpn. **51**, 3569 (1982).

[28]A. V. de Carvalho and S. R. Salinas, J. Phys. Soc. Jpn. **44**, 238 (1978).

[29]A. Levstik, C. Filipic, B. Zeks, R. Blinc, and H. Arend, J. Phys. C **19**, L25 (1986).

[30]R. C. Miller, Phys. Rev. **134**, A1313 (1964).

[31]F. Smuty and J. Fousek, Ferroelectrics **21**, 385 (1978).

[32]B. B. Lavrencic, M. Copic, M. Zgonik, and J. Petzelt, Ferroelectrics **21**, 325 (1978).

[33]Y. Tominaga, M. Kasahara, H. Urabe, and I. Tatsuzaki, Solid State Commun. **47**, 835 (1983).

[34]See the Raman spectra in the $X(ZZ)Y$ configuration in Ref. 35.

[35]Y. Tominaga, M. Tokunaga and I. Tatsuzaki, Jpn. J. Appl. Phys. **24**, Suppl. 24-2, 917 (1985).

[36]R. Blinc and B. Zeks, *Soft Modes in Ferroelectrics and Antiferroelectrics* (North-Holland, Amsterdam, 1974).

[37]T. Matsubara, Jpn. J. Appl. Phys. **24**, Suppl. 24-2, 1 (1985).

[38]N. Kojyo and Y. Onodera, J. Phys. Soc. Jpn. **57**, 4391 (1988).